Grinding surface roughness measurement based on the co-occurrence matrix of speckle pattern texture

Rong-Sheng Lu, Gui-Yun Tian, Duke Gledhill, and Steve Ward

Surface speckle pattern intensity distribution resulting from laser light scattering from a rough surface contains various information about the surface geometrical and physical properties. A surface roughness measurement technique based on the texture analysis of surface speckle pattern texture images is put forward. In the surface roughness measurement technique, the speckle pattern texture images are taken by a simple setup configuration consisting of a laser and a CCD camera. Our experimental results show that the surface roughness contained in the surface speckle pattern texture images has a good monotonic relationship with their energy feature of the gray-level co-occurrence matrices. After the measurement system is calibrated by a standard surface roughness specimen, the surface roughness of the object surface composed of the same material and machined by the same method as the standard specimen surface can be evaluated from a single speckle pattern texture image. The robustness of the characterization of speckle pattern texture for surface roughness is also discussed. Thus the surface roughness measurement technique can be used for an in-process surface measurement. © 2006 Optical Society of America

OCIS codes: 120.6660, 110.6150, 120.0120.

1. Introduction

Surface roughness measurement is very important for production quality control, for surface roughness of parts can significantly affect their friction, wear, fatigue, corrosion, tightness of contact joints, and positioning accuracy, etc. It has been investigated extensively to develop suitable techniques. The comprehensive reviews are contained in Refs. 1 and 2. Among them, the most common measurement techniques would be contact stylus, optical interferometry, microscopy, light scattering, laser speckle, etc., with the majority of them capable only of being used for off-line measurement. Stylus instruments, for example, are inherently slow in operation, though they yield accurate results, and may yield scratches on a surface, and optical interferometry and microscopy are often used for very fine surface off-line measurements. Fortunately, the measurement technique using light speckle techniques may be a good solution for on-line surface

roughness measurements. An instrument based on such a technique would offer an alternative to conventional mechanical stylus instruments to overcome their drawback and provide the means for automated in-process measurements.[3] Over the decades, since the invention of lasers, researchers have discussed the relationships between surface roughness and speckle pattern statistical properties as a new method for off-line as well as on-line surface measurements. Using the different properties of speckle fields and the different setup of optical systems, researchers have also developed a variety of speckle methods for surface roughness measurements. For instance, surface roughness measurements may be implemented by the speckle pattern illumination methods,[4,5] the speckle contrast methods,[6] and the speckle correlation methods.[7] Surface roughness measurement by means of speckle pattern illumination is convenient to determine rms roughness in the submicrometer range but requires a complicated optical illumination system consisting of a diffuser and a lens.[5] The speckle contrast methods, which are based on the first-order statistics of surface speckle patterns, can usually evaluate surface roughness values less than $R_a < 0.3$ μm. Speckle correlation methods, which are based on the second-order statistics of surface speckle patterns, may work on surface roughness R_a between 1 and 30 μm. However, they often need two speckle pattern images, which may be obtained by one of the follow-

R.-S. Lu (rslu@hfut.edu.cn) is with the School of Instrument Science and Opto-electronic Engineering, Hefei University of Technology, China. G.-Y. Tian, D. Gledhill, and S. Ward are with the School of Computing and Engineering, University of Huddersfield, UK.

ing methods: changing the incident light angle from the surface,[8] rotating the surface to be measured,[9] using two laser light beams.[10] Such correlation methods are difficult to use for the in-process surface roughness measurement of moving objects, except for using two-laser light illumination.

A surface speckle pattern, which is a grainy structure in the space produced by scattered light from a rough surface when illuminated by coherent light, contains rich information about the surface fine geometrical properties, such as the surface roughness. The speckle pattern images taken by an image sensor present texture form. The surface roughness information immersed in the speckle pattern images may be extracted by texture analysis. Surface roughness extraction by means of texture analysis has been explored by some researchers. Gadelmawla,[11] for example, has investigated the surface roughness characterization method using the gray level co-occurrence matrix of surface texture images, which are captured by a vision system. Chang and Ravathur[12] characterized surface roughness from the texture images of very roughened surfaces using multiresolution wavelet decomposition. The surface roughness R_a range in their experimental investigation covers ~20–600 μm. Other surface roughness characterization methods by means of surface texture image analysis are contained in Refs. 13–16. However, very little literature about surface roughness characterization, directly from speckle pattern texture images using texture analysis, can be found.

In this paper, we will investigate the statistical properties of speckle pattern texture from the point of view of computer texture analysis and introduce a simple method for characterizing a grinding object's surface roughness from a single laser speckle pattern image, which is taken by a simple configuration setup consisting of a laser and a CCD camera. The surface roughness is extracted by using the gray-level co-occurrence matrix (GLCM) of the speckle pattern texture image and quantized by the features of the GLCM. Though there are many parameters that can be used to characterize surface roughness, this paper will concentrate on the relationship of the parameter R_a with the GLCM from speckle images due to the paper length limitation. The merit of the surface roughness evaluation method depicted in the paper is that it is easily carried out and is useful for in-process surface roughness inspection.

2. Theory and System Setup Configuration

The basic configurations of the setup for surface roughness measurements by means of speckle pattern images are shown in Fig. 1. In Fig. 1(a), the speckle pattern formed in free-space geometry is called objective speckle. Alternatively, the speckle pattern that is formed by collecting the scattered light with a lens and focusing it onto a screen is called subjective speckle pattern as shown in Fig. 1(b). The
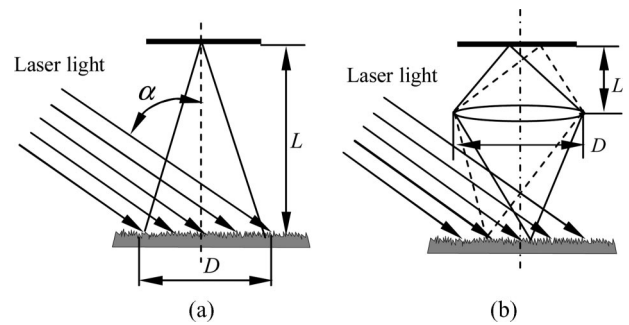

Fig. 1. Basic schemes of the speckle pattern formation and the experimental setup.

size of speckles, a statistical average of the distance between adjacent regions of maximum and minimum intensity is given by[17]

$$z = 1.22\lambda\rho\frac{L}{D}, \qquad (1)$$

where λ is the wavelength of the laser light, $\rho = 1$ for objective speckles, and $\rho = (1 + M)$ for subjective speckles, where M is the lens magnification. Other geometrical parameter meanings are shown in Fig. 1.

In our research, we adopt the Fig. 1(a) setup configuration for convenience, to obtain a proper size of speckle pattern and investigate the influence of the distance L variations on surface roughness evaluation. The setup is built with a digital camera and a 35 MW diode laser with a wavelength of 660 μm, the power of which can be adjusted to avoid the digital camera signal saturation. The camera is located in the specimen normal direction. The angle between the incident laser light beam and the normal direction is fixed to be as small as practically possible to reduce the effect of the direction of surface micostructure in the surface roughness evaluation. In the setup, the angle is ~10°. By means of the simple setup, different speckle pattern images from standard grinding surface roughness specimens are obtained. The speckle pattern texture images against
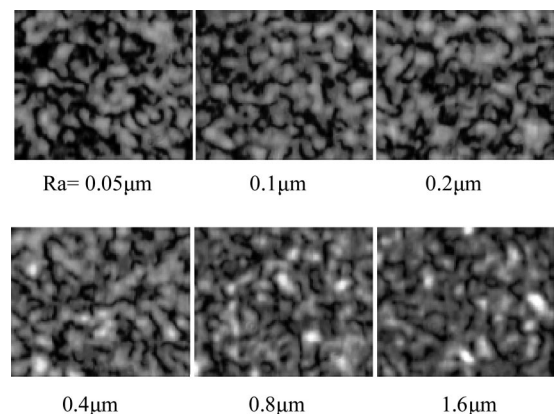

Ra= 0.05μm   0.1μm   0.2μm

0.4μm   0.8μm   1.6μm

Fig. 2. Speckle pattern variations against the specimen surface roughness.

surface roughness R_a values are shown in Fig. 2. From left to right of the images, it is apparent that the speckle pattern contrast becomes weaker and the image signal approaches saturation with the surface roughness R_a increasing. This implies that the speckle pattern texture properties change with the surface roughness, and it is possible to extract the surface roughness from the speckle pattern texture images using texture analysis.

3. Computation of the Speckle Pattern Texture Co-occurrence Matrix

Information extraction from texture images can be accomplished by different texture analysis methods, which are classified into four categories: statistical methods, geometrical methods, model-based methods, and signal processing methods.[18] A discussion of their relationships and applications are given in Ref. 19, including a second-order statistics feature for texture representation.[20] Here we will investigate the surface roughness evaluation method using the gray-level co-occurrence matrix, which belongs to the statistical methods. The reason it is chosen is that the gray-level co-occurrence matrix is based on second-order statistics, which deal with the spatial relationships of pairs of gray values of pixels in texture images.

The texture image gray-level co-occurrence matrix indicates how often pairs of gray levels of pixels, which are separated by a certain distance and lie along a certain direction, occur in a texture image, as defined in Ref. 21. Let a digital texture image be $f : L_x \times L_y \to G$, with horizontal and vertical spatial domains: $L_x = \{0, 1, \ldots, n_x\}$ and $L_y = \{0, 1, \ldots, n_y\}$, respectively, and the gray levels $G = \{0, 1, \ldots, m - 1\}$. Let an offset d be the distance that separates two pixels, whose positions are (x_1, y_1) and (x_2, y_2), respectively, and whose gray values are i and j, respectively. $d = 1$ means the pixel pairs are neighboring pixels, $d = 2$ means pixel pairs are separated by one pixel, and so forth. If giving four angles (directions) of $\theta = 0°, 45°, 90°,$ and $135°$ as shown in Fig. 3, along which the pairs of pixels lie, thus for a fixed offset distance d, one obtains the four co-occurrence matrices P_0, P_{45}, P_{90}, and P_{135}, which are defined as follows:

$$P_0 = [p_0(i, j)], \quad i = 0, \ldots, m - 1, \quad j = 0, \ldots, m - 1, \tag{2}$$

where $p_0(i, j)$ is the cardinality of the set of pixel pairs having the properties that

$$f(x_1, y_1) = i, \qquad f(x_2, y_2) = j,$$

$$|x_1 - x_2| = d, \qquad y_1 = y_2. \tag{3}$$

For the definition of P_{45}, one has to replace condition (3) by

$$\{(x_1 - x_2 = -d) \wedge (y_1 - y_2 = -d) \vee (x_1 - x_2 = d)$$

$$\wedge (y_1 - y_2 = d). \tag{4}$$

The computational example of the gray-level co-occurrence matrix P_0 is illustrated in Fig. 4, where the image size $n_x \times n_y = 4 \times 5$, maximum gray level $m - 1 = 7$, and offset $d = 1$.

A co-occurrence matrix is capable of texture analysis by using texture features extracted from GLCM. Haralick *et al.*[21] suggested 14 textural features that can be used. Here, we chose four features, contrast, correlation, energy, and homogeneity, for speckle pattern texture analysis. The contrast feature measures the local variations in the gray-level co-occurrence matrix; correlation measures the joint probability occurrence of the specified pixel pairs; energy, which is also known as uniformity or the angular second moment, provides the sum of squared elements in the GLCM; and homogeneity measures the closeness of the distribution of elements in the GLCM to the GLCM diagonal. They are defined as follows:

$$P_{\mathrm{normalized}} = [p'(i, j)] = \frac{1}{\sum\limits_{i=0}^{m-1} \sum\limits_{j=0}^{m-1} p(i, j)} [p(i, j)], \tag{5}$$

then the four features are

$$\text{Contrast:} \quad \sum_{i=0}^{m-1} \sum_{j=0}^{m-1} |i - j|^2 p'(i, j), \tag{6}$$

$$\text{Correlation:} \quad \sum_{i=0}^{m-1} \sum_{j=0}^{m-1} \frac{\left[i - \sum\limits_{i=0}^{m-1} \sum\limits_{j=0}^{m-1} j p'(i, j) \right]\left[j - \sum\limits_{i=0}^{m-1} \sum\limits_{j=0}^{m-1} i p'(i, j) \right] p'(i, j)}{\sqrt{\sum\limits_{i=0}^{m-1} \sum\limits_{j=0}^{m-1} (j - u_i)^2 p'(i, j)} \sqrt{\sum\limits_{i=0}^{m-1} \sum\limits_{j=0}^{m-1} (i - u_j)^2 p'(i, j)}}, \tag{7}$$

$$\text{Energy:} \quad \sum_{i=0}^{m-1} \sum_{j=0}^{m-1} p'(i, j)^2, \tag{8}$$

$$\text{Homgeneity:} \quad \sum_{i=0}^{m-1} \sum_{j=0}^{m-1} \frac{p'(i, j)}{1 + |i - j|}. \tag{9}$$
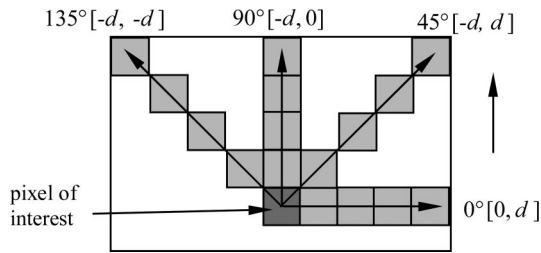
Fig. 3.   Co-occurrence matrix offset and its direction definition.

Considering the speckle pattern texture distribution in images is not homogeneous in all directions, let us compute the gray-level co-occurrence matrix of the speckle pattern texture images in the following four directions with offset distance d as

that the periods are the same and do not change with surface roughness. Each triangular waveform is also modulated by an exponential component. The curves of co-occurrence statistic energy and homogeneity also show that the triangular waveforms severely vibrate at the beginning but attenuate with the periods. They become stable after 10 periods that correspond to 20 pixel offsets in the speckle pattern texture images. The feature curves have not directly presented their relationships with the surface roughness of the samples. To be able to quantify the surface roughness from the texture feature, our experimental results show that the exponential component parameters of the energy feature have a good relation to the surface roughness in contrast to the other three feature curves. The exponential component parameters

$$
\begin{aligned}
\text{offsets}[0, \ d] &= [0 \ 1; \ \ 0 \ 2; \ \ 0 \ 3; \ \ 0 \ 4; \ \ \ldots; \ \ 0 \ 60], \\
\text{offsets}[45, \ d] &= [-1 \ 1; \ \ -2 \ 2; \ \ -3 \ 3; \ \ -4 \ 4; \ \ \ldots; \ \ -60 \ 60], \\
\text{offsets}[90, \ d] &= [-1 \ 0; \ \ -2 \ 0; \ \ -3 \ 0; \ -4 \ 0; \ \ \ldots; \ \ -60 \ 0], \\
\text{offsets}[135, \ d] &= [-1 \ -1; \ \ -2 \ -2; \ \ -3 \ -3; \ \ -4 \ -4; \ \ \ldots; \ \ -60 \ -60]
\end{aligned}
$$

and set the image gray-value scaling factor $m = 256$ to obtain maximum information. For each offset $[\theta, d]$ array and each texture feature in Eqs. (7)–(9), 60 feature values are obtained. If drawing the values of each feature in the four directions into the same diagram, four diagrams indicating the relationship of the features contrast, correlation, energy, and homogeneity with the offsets are obtained. Figure 5 illustrates the computational results, which are obtained from the image of a grinding surface with roughness $R_a = 0.1 \ \mu$m, shown in Fig. 2. To clarify the diagrams, each direction curve in the same diagram is separately plotted with a certain offset in the ordinate direction.

4. Surface Roughness Extraction from Texture Features

In the Fig. 5 feature diagrams, it is apparent that all four feature curves have periodical triangular waveform components. Our experimental results show
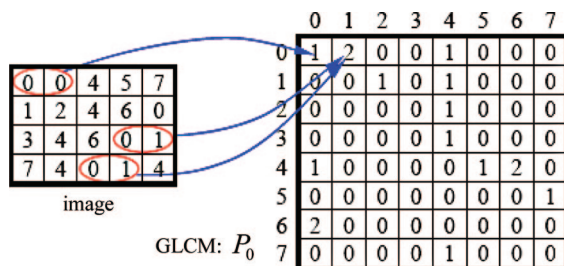
can be obtained by fitting the energy feature curves in the four directions with the following curve equation:

$$
y = y_0 + k \, \exp(-x/\sqrt{\sigma}), \tag{10}
$$

where x indicates the offset distance d and y is the energy feature value.

As Fig. 5 shows, in different directions the triangular waveforms have different amplitudes and offsets. This implies that the shapes of speckle patterns are not uniformly distributed in the four directions. Computation of invariant features is mostly done either by using moments, through harmonic analysis, or by using the autocorrelation function (ACF).[22] In contrast, a feature normalization technique is applied.[23] To reduce the influence of the variances of the amplitudes and offsets, before computing the exponential component parameters, the energy feature curves in the four directions are normalized by

$$
y' = \frac{y - u_y}{\sigma_y}, \tag{11}
$$

where u_y and σ_y indicate the mean value and standard deviation of the feature curve value y. The normalized energy feature curves of the speckle pattern texture with roughness $R_a = 0.1 \ \mu$m are illustrated in Fig. 6. The fitting exponential curve is also drawn in the same figure. For speckle pattern texture images from specimens with different surface roughnesses shown in Fig. 2, different fitting results can be ob-
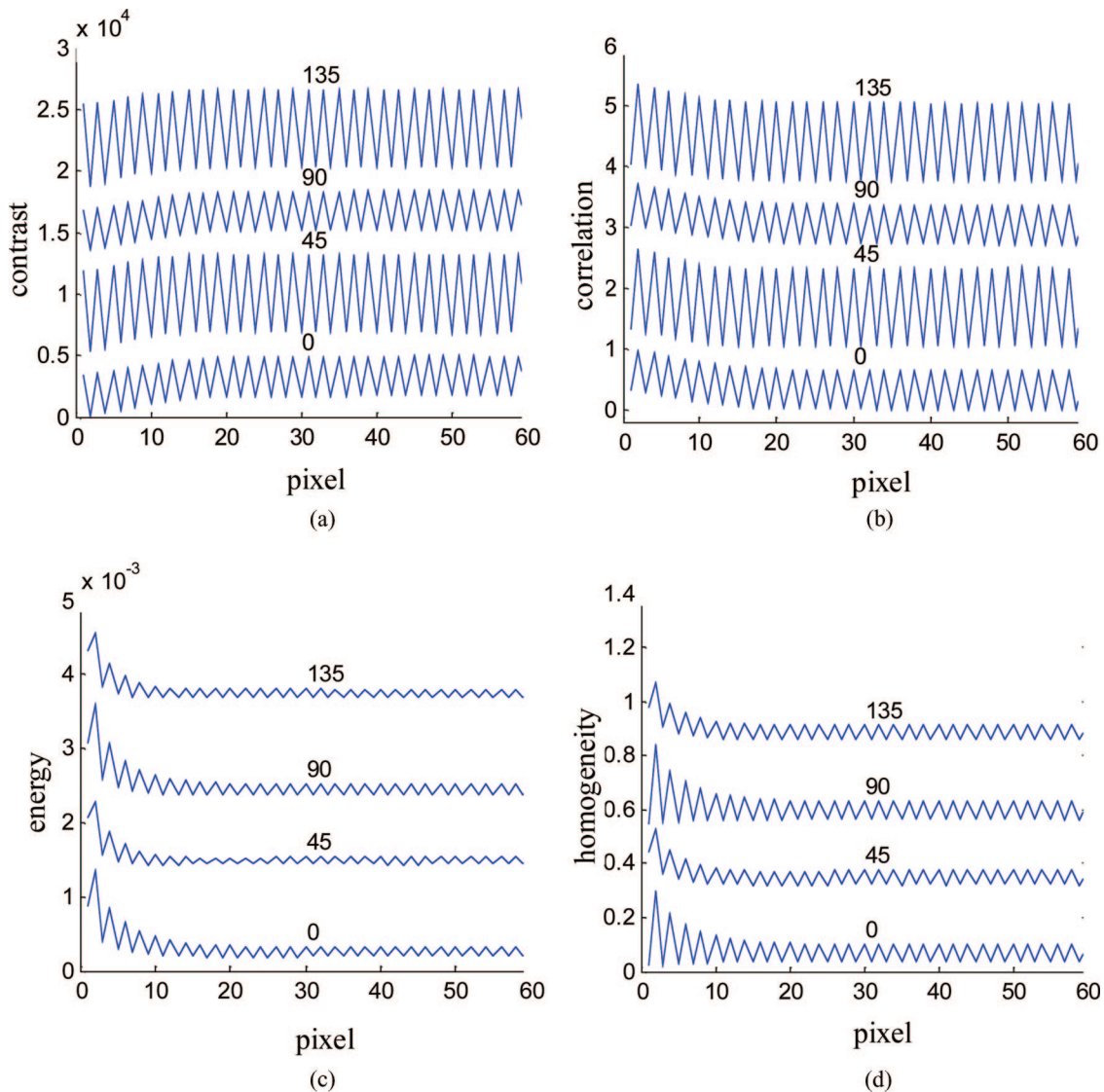

Fig. 4.   (Color online) Illustration of gray-level co-occurrence matrix computation.

Fig. 5.   (Color online) Feature curves of the speckle pattern texture of the specimen surface with $R_a = 0.1$ μm.

tained. If plotting the fitting parameters against surface roughness, their relationship curves can be obtained, which are illustrated in Fig. 7. To demonstrate the effects of the normalization and nonnormalization fitting results of the energy feature curves

Fig. 6.   (Color online) Energy feature curves normalization.

on surface roughness evaluation, in Fig. 7 two kinds of computational result curves are plotted. In the following sections, we will discuss the robustness of the fitting parameters under different measurement conditions and identify which one is the best to characterize surface roughness.

5. Robustness of the Surface Roughness Evaluation

To test the robustness of the surface roughness evaluation method above, in this section, we will investigate the influences of the setup configuration variances, such as the laser light power, surface machining mark directions, and the distance of the surface to the observation plane.

A. Influence of the Laser Power Variance

In the setup configuration shown in Fig. 1(a), the camera is a digital camera, JAI CV-M8CL. The range of gray-level image signal coming from the camera is set from 0 to 255. The speckle pattern images result from
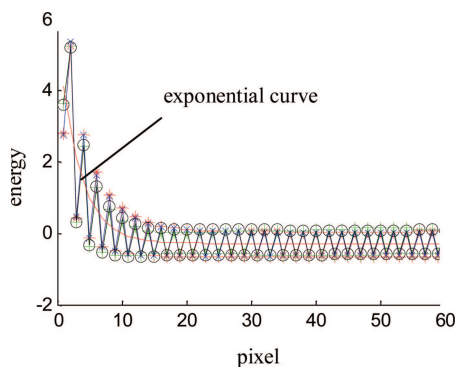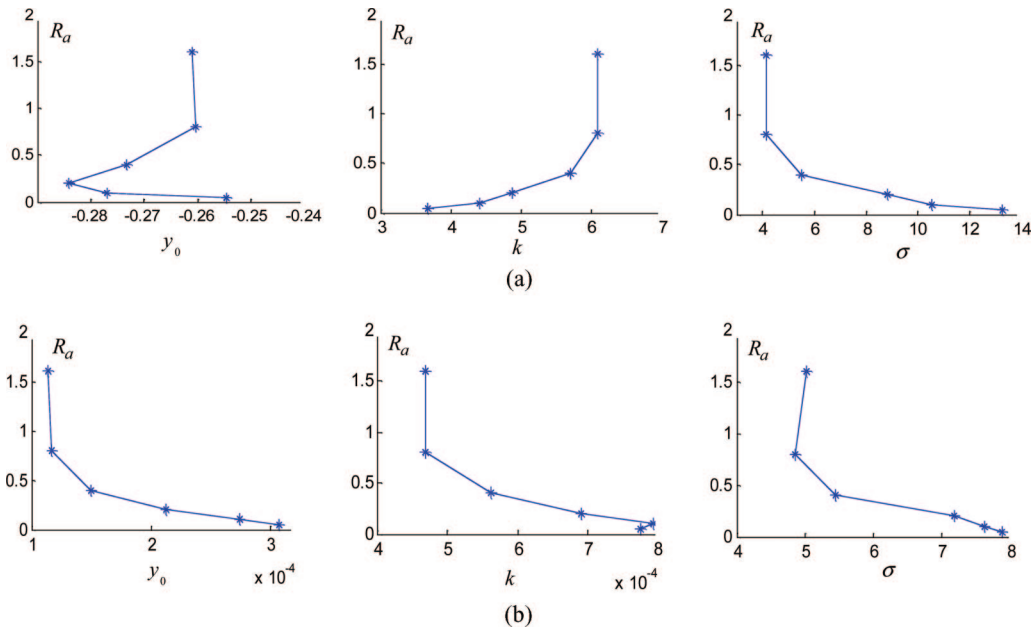
Fig. 7. Relationship between surface roughness and energy feature curve-fitting parameters. (a) Normalized computational results, (b) nonnormalized computational results.

the laser light scattering near the surface normal direction. For a rougher surface, more scattered laser light goes into the camera and results in brighter speckle images. To avoid the digital camera signal being saturated by the strong scattered laser light, the laser power should be set so that the largest image gray-level value coming from the roughest surface to be measured, such as the specimen surface with $R_a = 1.6$ μm in our experiment, is less than 255.

To test the influence of the laser light power variance, the serial speckle pattern texture images resulting from a certain surface are captured by changing the laser light power. Figure 8 shows a small portion of texture images captured from the specimen surface with roughness $R_a = 0.1$ μm. The number beneath each texture image indicates the maximum image gray-level value in the corresponding image after changing the laser light power. Based on the images and the surface roughness extraction method de-
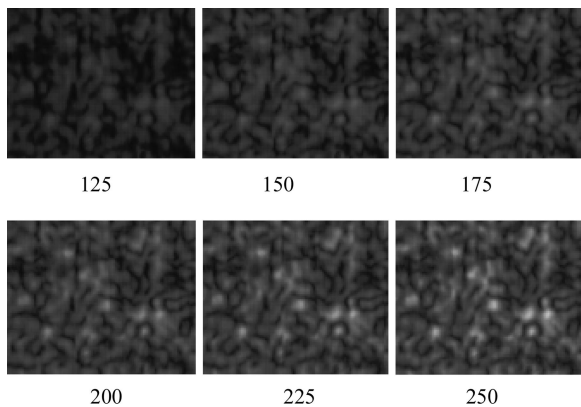

Fig. 8. Speckle pattern texture images influenced by laser light power.

picted above, the exponential parameters of the energy features of the texture image gray-level co-occurrence matrix of each speckle texture image are calculated. Figure 9 illustrates the relationship between the exponential parameters and the maximum image level.

Figure 9 shows that exponential parameter variances caused by the unstable laser power is significant during lower laser power illumination. When the maximum gray-level value of the texture images is larger than 175, the parameter variances become smaller. To compare the influence when the maximum image gray-level value changes between 175 and 250, Table 1 lists the statistical computational results of the exponential parameters, their mean values, standard deviations, and the percents of the deviations against the mean values. To find which parameter is the best one to formulate the surface roughness, it is reasonable to compare the ratio of the standard deviation against the mean value in each column of Table 1. From Table 1, it is obvious that normalized parameter k is more stable with respect to the change of the laser power. Though the ratio value of the deviations against the mean values of the normalized exponential curve parameter absolute value, y_0, is smallest, the parameter is incapable of formulating surface roughness, as shown in Fig. 9(a).

B. Influence of the Surface Distance

For different surfaces to be measured, the distance L between the surface and the image plane of the CCD camera, as shown in Fig. 1, may be difficult to keep constant, particularly in on-line inspection. To investigate the influence of the distance variance on the surface roughness evaluation, a series of speckle pat-
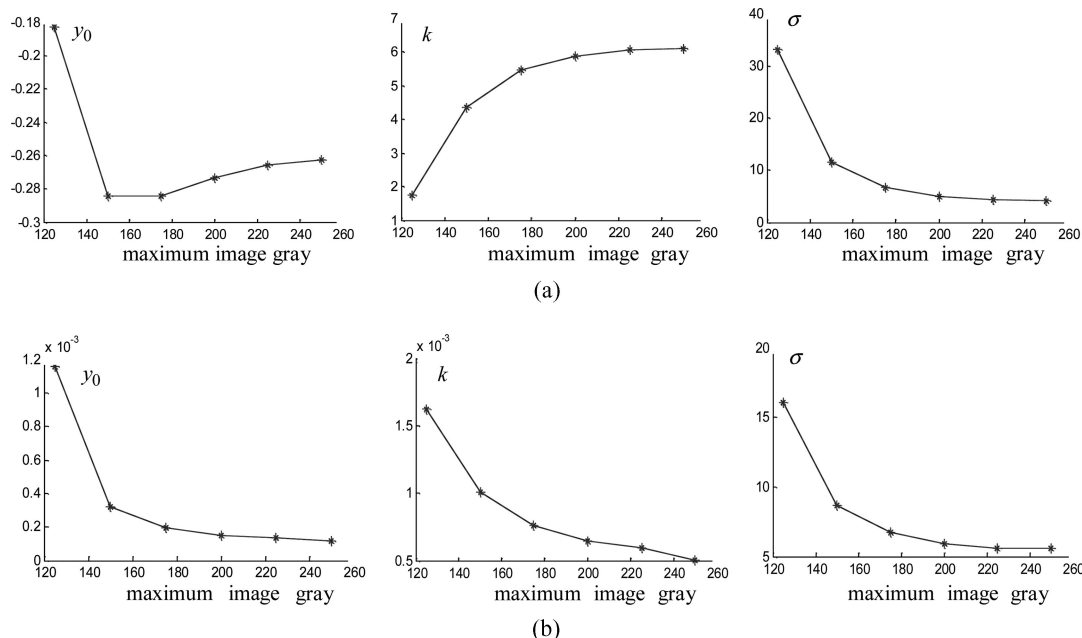
Fig. 9. Influence of the laser power on the energy texture feature. (a) Normalized computational results, (b) nonnormalized computational results.

tern texture images at different distance variances from 0 to 1 mm at the 150 mm original distance are taken. Then, to compute the relationship of the exponential parameters of the energy feature with the distance variances use the same method as depicted in Section 4. The curves indicating energy features against distance variance and their statistical results are illustrated in Fig. 10 and Table 2. From Table 2, it can be found that the influence of the distance variance is very tiny compared with the influences of laser power variances, and the energy feature normalized parameter k is more stable, without considering the smallest ratio value between the deviation and the mean values of the normalized exponential curve parameter absolute value y_0.

C. Influence of Machining Orientations

Most object surfaces machined in workshops have regular machining mark distribution. When the incident laser light shown in Fig. 1(a) is obliquely projected on the surface to be measured, the scattered light distribution near the surface normal direction will depend on the machining mark ori-

entation against the incident light. The speckle pattern texture images captured by the digital camera in Fig. 1(a) will change with the machining mark orientation. To investigate the influence of the orientation variance on surface roughness evaluation, a grinding surface specimen is rotated from 0° to 90°, and serial speckle pattern texture images are taken by the digital camera. Then, the energy feature extraction is done as depicted in Subsection 5.A, and the exponential fitting parameter curves against the rotation angle are obtained. Table 3 shows the statistical values of with and without normalized techniques for feature fitting curves. The normalized parameter k seems more stable. It is inconclusive for the variations of machining directions. Comprehensive study for different manufacturing direction samples with different R_a will be undertaken in the future.

6. Discussion

In the depiction in Section 5, it can be found that in the common four texture features extracted from

Table 1. Influence of the Laser Power on the Energy Texture Feature

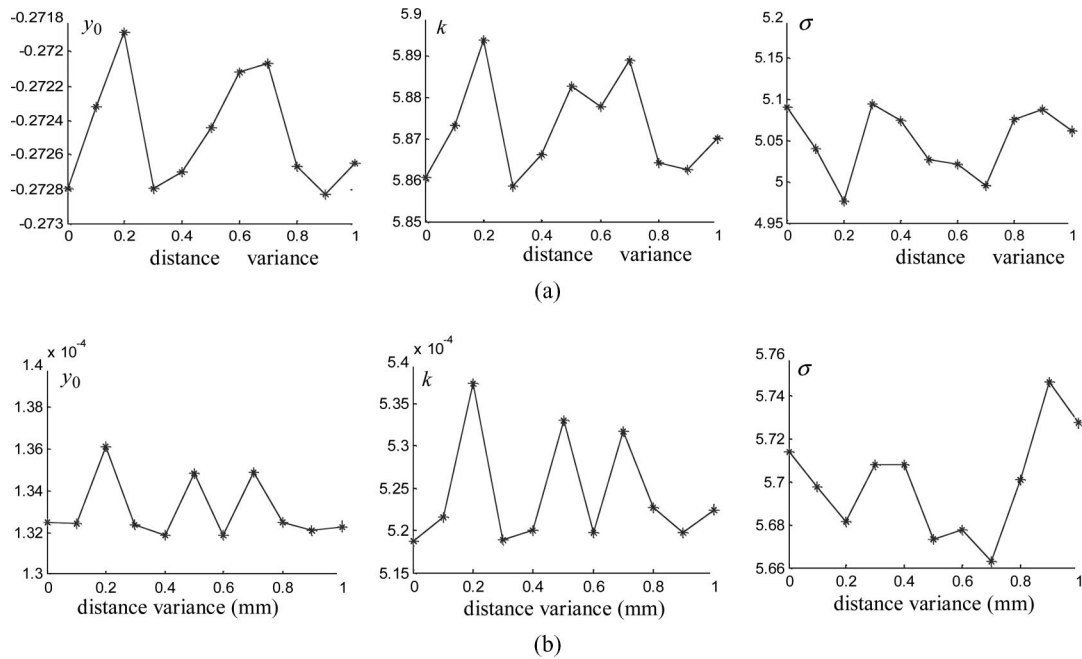| Gray Level | Normalized | | | Nonnormalized | | |
	y_0	k	σ	$y_0 \times 10^{-4}$	$k \times 10^{-4}$	σ
175	−0.28	5.46	6.73	1.92	7.60	6.75
200	−0.27	5.88	5.08	1.51	6.42	5.91
225	−0.26	6.06	4.38	1.36	5.93	5.58
250	−0.26	6.11	4.16	1.17	5.03	5.63
Mean	−0.27	5.88	5.09	1.49	6.25	5.97
Standard deviation	0.008	0.56	1.01	0.28	0.93	0.47
Standard deviation/mean	−3.09%	4.35%	19.80%	18.61%	14.85%	7.82%

Fig. 10. Influence of the distance L variance on the energy texture feature. (a) Normalized computational results, (b) nonnormalized computational results.

the gray-level co-occurrence matrix of speckle pattern texture images, only the normalized curve parameters, k and σ, and the nonnormalized curve parameters, y_0, k, and σ, of the exponential trend of the energy feature waveform have a good relationship with surface roughness. Based on the investigation of their robustness against the variances of laser power, surface distance, and surface microstructure, however, it is apparent that the normalized exponential curve parameter k is more stable than the others in each case. Therefore the normalized exponential curve parameter k is the best one that can be used to characterize surface roughness. The investigation in Section 5 also shows that both the variances of the laser light power and the surface microstructure orientation have significant influence. It can be

overcome by using normalized feature fitting as introduced in Subsection 5.A. In addition to feature normalization, to deal with the influence of the surface microstructure, the oblique angle of the incident laser light should be set as small as practical. If we insert a splitter on the way between the camera and the surface to be measured and let the laser light beam emit on the surface vertically, the influence may be removed. The investigation in Subsection 5.B also shows that the influence of the surface distance to the camera image plane during a 1 mm small range is negligible. This property makes the surface roughness measurement method very effective for the in-process surface measurement in the circumstance where the surface position is interrupted by vibrations.

Table 2. Influence of the Distance Variance on the Energy Texture Feature

	Normalized			Nonnormalized		
	y_0	k	σ	$y_0 \times 10^{-4}$	$k \times 10^{-4}$	σ
Mean	−0.27	5.87	5.05	1.33	5.24	5.70
Standard deviation	0.0003	0.011	0.04	0.01	0.06	0.23
Standard deviation/mean	0.12%	0.19%	0.76%	1.57%	1.19%	0.41%

Table 3. Influence Caused by the Surface Microstructure Orientations

	Normalized			Nonnormalized		
	y_0	k	σ	$y_0 \times 10^{-4}$	$k \times 10^{-4}$	σ
Mean	−0.28	5.46	6.72	1.53	5.69	6.37
Standard deviation	0.003	0.16	0.63	0.14	0.37	0.34
Standard deviation/mean	1.19%	3.01%	9.38%	9.03%	6.50%	5.34%

7. Conclusion

We have put forward a surface roughness measurement technique through investigating the relationship between the surface speckle pattern texture and the features of the texture image gray-level co-occurrence matrix. There are many texture features that can be extracted from the gray-level co-occurrence matrix. In our research, the four commonly used features—contrast, correlation, energy, and homogeneity—are studied with respect to surface roughness. As discussed, the parameter k of the normalized exponential trend curve of the energy feature has a good relationship with the surface roughness; is more robust to the variances of the setup configuration, the position, and the orientation of the surface to be measured; and is the best feature parameter to characterize the surface roughness.

From the experimental results with the grinding surface roughness specimens, the surface roughness measurement technique is effective to characterize the grinding surface roughness from $R_a = 0.05$ μm to $R_a = 1.6$ μm. For different object surfaces consisting of specific material and machined by specific methods, the range of the surface roughness, which can be characterized by the method, may be different. This means the surface roughness measurement technique we have developed needs calibration beforehand.

In the surface roughness measurement technique, the speckle pattern texture images are taken by a very simple setup configuration consisting of a laser and a CCD camera. The parameter k of the exponential trend of the energy feature for a specific object surface is computed from only a single speckle pattern texture image of the surface. This means, after the measurement system is calibrated by standard specimen surfaces, that the surface roughness of the object surface composed of the same material and machined in the same way as the standard specimen surfaces can be evaluated from a single speckle pattern texture image. The co-occurrence matrix feature is only one of the texture features. More features and their fusion will be investigated under different manufactured samples versus different roughness parameters including R_a. In collaboration with the normalization techniques, the surface roughness measurement technique can be used for in-process surface measurements.

References

1. D. J. Whitehouse, *Handbook of Surface and Nanometrology* (Institute of Physics, 2003).
2. J. M. Bennet and L. Mattsson, *Introduction Surface Roughness and Scattering* (Optical Society of America, 1993).
3. B. Ruffing, "Application of speckle-correlation methods to surface-roughness measurement: a theoretical study," J. Opt. Soc. Am. A **3,** 1297–1304 (1986).
4. T. Yoshimura, K. Kato, and K. Nakaeawa, "Surface roughness dependence of the intensity correlation function under speckle pattern illumination," J. Opt. Soc. Am. A **7,** 2254–2259 (1990).
5. P. Lehmann, "Surface-roughness measurement based on the intensity correlation function of scattered light under speckle-pattern illumination," Appl. Opt. **38,** 1144–1152 (1999).
6. L. C. Leonard and V. Total, "Roughness measurement of metallic surfaces based on the laser speckle contrast method," Opt. Lasers Eng. **30,** 433–440 (1998).
7. C. Cheng, C. Liu, N. Zhang, T. Jia, R. Li, and Z. Xu, "Absolute measurement of roughness and lateral-correlation length of random surfaces by use of the simplified model of image-speckle contrast," Appl. Opt. **41,** 4148–4156 (2002).
8. G. S. Spagnolo, D. Paoletti, A. Paoletti, and D. Ambrosini, "Roughness measurement by electronic speckle correlation and mechanical profilometry," Measurement **20,** 243–249 (1997).
9. S. L. Toh, C. Quan, K. C. Woo, C. J. Tay, and H. M. Shang, "Whole field surface roughness measurement by laser speckle correlation technique," Opt. Laser Technol. **33,** 427–434 (2001).
10. C. Joenathan, R. Torroba, and R. Henao, "Surface roughness effects in dual beam illumination speckle interferometers—theoretical study," Optik **112,** 163–158 (2001).
11. E. S. Gadelmawla, "A vision system of surface roughness characterization using the gray level of co-occurrence matrix," NDT & E Int. **37,** 557–588 (2004).
12. S. I. Chang and J. S. Ravathur, "Computer vision based on no-contact surface roughness assessment using wavelet transform and response surface methodology," Qual. Eng. **17,** 435–451 (2005).
13. R. Kumar, P. K. Kulashekar, B. Dhanasekar, and B. Ramamoorthy, "Application of digital image magnification for surface roughness evaluation using machine vision," Int. J. Mach. Tools Manuf. **45,** 228–234 (2005).
14. M. B. Kiran, B. Ramamoorthy, and V. Radhakrishnan, "Evaluation of surface roughness by vision system," Int. J. Mach. Tools Manuf. **38,** 685–690 (1998).
15. G. A. Al-kind, R. M. Baul, and K. F. Gill, "An application of machine vision in the automated inspection of engineering surfaces," Int. J. Prod. Res. **30,** 241–253 (1992).
16. C. Lee and Y. J. Chao, "Surface texture dependence on surface roughness by computer vision," in *IEEE International Conference on Robotics and Automation* (IEEE, 1987), Vol. 4, pp. 520–524.
17. J. C. Dainty, ed., *Laser Speckle and Related Phenomena,* Vol. 9 of Topics in Applied Physics (Springer-Verlag, 1984).
18. M. Tuceryan and A. K. Jain, "Texture analysis," in *Handbook of Pattern Recognition and Computer Vision,* 2nd ed., C. H. Chen, L. F. Pau, and P. S. P. Wang, eds. (World Scientific, 1998), pp. 207–248.
19. X. Liu and D. Wang, "Texture classification using spectral histograms," IEEE Trans. Image Process. **12,** 661–570 (2003).
20. S. H. Ryu, D. K. Choi, and C. N. Chu, "Roughness and texture generation on end milled surfaces," Int. J. Mach. Tools Manuf. **46,** 404–412 (2006).
21. R. M. Haralick, K. Shanmugam, and I. Dinstein, "Texture features for image classification," IEEE Trans. Syst. Man Cybern. **3,** 610–621 (1973).
22. J. Brochard, M. Khoudeir, and B. Augereau, "Invariant feature extraction for 3D texture analysis using the autocorrelation function," Pattern Recogn. Lett. **22,** 759–768 (2001).
23. G. Finlayson, S. Hordley, G. Schaefer, and G. Y. Tian, "Illuminant and device invariant colour using histogram equalization," Pattern Recogn. **38,** 179–190 (2005).